Ab initio Electronic Structure of Liquid Water

Wei Chen,* Francesco Ambrosio, Giacomo Miceli, and Alfredo Pasquarello
Chaire de Simulation à l'Echelle Atomique (CSEA), Ecole Polytechnique Fédérale de Lausanne (EPFL), CH-1015 Lausanne, Switzerland
(Received 15 December 2015; published 24 October 2016)

Self-consistent *GW* calculations with efficient vertex corrections are employed to determine the electronic structure of liquid water. Nuclear quantum effects are taken into account through *ab initio* path-integral molecular dynamics simulations. We reveal a sizable band-gap renormalization of up to 0.7 eV due to hydrogen-bond quantum fluctuations. Our calculations lead to a band gap of 8.9 eV, in accord with the experimental estimate. We further resolve the ambiguities in the band-edge positions of liquid water. The valence-band maximum and the conduction-band minimum are found at −9.4 and −0.5 eV with respect to the vacuum level, respectively.

DOI: 10.1103/PhysRevLett.117.186401

Liquid water is such a ubiquitous substance that it has been the subject of upsurging research efforts for the past 30 years. Of particular importance is the electronic structure of liquid water, the significance of which has been recently highlighted in clean-energy technologies through semiconductor-assisted artificial photosynthesis [1,2]. A good understanding of the electronic structure of water is a prerequisite toward the design of photocatalytic systems with high catalytic activity.

The extended hydrogen-bond network of liquid water gives rise to the formation of electronic bands. The valence band maximum (VBM) is characterized by the localized $2p_z$ electrons of O atoms. The conduction band minimum (CBM) derives from the antibonding orbitals of O–H bonds, and is at variance much more extended. Experimentally determined positions of these band edge states have yet to reach a consensus. Early ultraviolet (UV) photoemission experiments by Delahay and collaborators reported photoemission threshold energies of 9.3 [3] and 10.06 eV [4]. More recent work by Winter *et al.* employed the liquid microjet technique and found a threshold energy of 9.9 eV [5]. For the unoccupied states, inverse photoemission and photoionization measurements placed the CBM at −1.2 eV with respect to the vacuum level [6,7]. This value was later revised to −0.74 eV, in light of the observation that excess electrons in liquid water could be initially captured in a localized trap state below the actual CBM [8]. Altogether, these measurements allude to a band gap of 8.7 eV, but associated with a sizable uncertainty of ±0.6 eV.

To shed light on the electronic structure of water, it is necessary to resort to a fully *ab initio* method, which avoids the use of experimental input. *Ab initio* molecular dynamics (MD) simulations based on Kohn-Sham density-functional theory (DFT) have been extensively carried out to understand the structural and dynamical properties of water and of aqueous solutions. It is well recognized that the use of semilocal density functionals precludes a faithful description of the electronic structure and the predicted band gap of liquid water is apparently too small [9,10]. Hybrid functionals improve the description of the electronic structure [10], but the mixing parameter of the Fock exchange is not known *a priori* without the input from experiment or higher levels of theory. Many-body perturbation theory based on Hedin's *GW* approximation [11], is a more rigorous approach to the problem of electronic excitations. As the *GW* method is computationally demanding, one-shot or partial self-consistent calculations are usually performed for aqueous solutions [12–18]. However, these calculations are tied to the specific choice of the starting point, and band gaps varying between 7.3 to 9.5 eV have been reported for liquid water [12–15,17]. The quasiparticle self-consistent *GW* (QS*GW*) method shows no dependency on the starting point [19,20], but in this scheme vertex corrections are imperative to achieve accurate band gaps [21,22]. The inclusion of vertex corrections has yet been elusive for large-scale systems.

On the more fundamental side, light protons make the hydrogen-bond network susceptible to quantum fluctuations. The inclusion of nuclear quantum effects (NQEs) noticeably modifies the structural and dynamical properties of liquid water [23–29]. In the context of the electronic structure, the quantum zero-point motion of nuclei renormalizes the electronic band gap [30–39]. As a consequence, quantum effects play an integral part in the description of the electronic structure of liquid water, but very often their importance is underappreciated in *ab initio* MD simulations.

In this Letter, we report the electronic structure of liquid water as obtained through state-of-the-art self-consistent QS*GW* combined with path-integral *ab initio* MD simulations. Our self-consistent *GW* method includes vertex corrections in the screened interaction, which are made efficient by the recently adapted [40] bootstrap exchange-correlation kernel f_{xc} [41]. The high accuracy of the method has been demonstrated for various materials [40]. NQEs are incorporated in the path-integral formalism in which the partition function of the quantum system is

mapped onto the classical one of a ring polymer, with its "beads" coupled via harmonic springs [42]. Within the present scheme, we reach excellent agreement with the experimental photoemission spectra. The calculated band gap (8.9 eV) and band-edge positions further support the experimental assignment. Such an agreement is achieved only when vertex corrections and NQEs are both taken into account.

Ab initio path-integral MD simulations in the canonical *NVT* ensemble are performed with the i-PI wrapper for the nuclear degrees of freedom [43], with interatomic forces fed through DFT calculations using the QUANTUM-ESPRESSO code [44]. We use a generalized Langevin equation thermostat [45], which ensures the convergence with as few as six beads for liquid water [46,47]. As a first step, MD trajectories with classical nuclei are collected over a production run of 10 ps following an equilibration of 5 ps with a stochastic velocity rescaling thermostat [48]. Starting from the final configurations of classical water, our simulations with quantum nuclei run for 10 ps, with the first 2 ps discarded for equilibration [49]. All MD simulations use an integration time step of 0.5 fs. We focus on simulations at ambient temperature (300 K). Extended simulations at 350 and 400 K are also performed to investigate the temperature dependence of the electronic structure. Norm-conserving pseudopotentials with a plane-wave cutoff of 85 Ry are used in the DFT calculations. To account for the nonlocal van der Waals dispersion, which is critical for the hydrogen-bond network [50,51,60–63], the revised Vydrov and Van Voorhis (rVV10) van der Waals density functional [52,53] is used in the MD simulations. The short-range behavior is controlled by an empirical parameter b in the rVV10 density functional [52,53]. To ensure a liquidlike state at room temperature while maintaining a realistic equilibrium density of water, we choose $b = 8.9$ [49]. Nevertheless, the electronic structure is robust against the choice of b insofar as the water is not in a glassy state [49]. Liquid water is modeled by 32 water molecules contained in a cubic supercell of length 9.82 Å, closely matching the experimental density. The sole Γ point of the Brillouin zone is sampled in the MD simulations.

The calculated radial distribution functions (cf. Fig. 1) show that NQEs soften the structure of water and generally improve the agreement with scattering experiments [64]. NQEs are most noticeable for the oxygen-hydrogen and hydrogen-hydrogen distribution functions (g_{OH} and g_{HH}), whereas the oxygen-oxygen distribution g_{OO} is less affected [29]. In particular, the first two peaks of g_{OH} correspond to the intramolecular covalent O–H bond and the intermolecular O $\cdots$ H hydrogen bond, and their broadening implies a higher likelihood of proton transfer [49].

The hydrogen-bond fluctuations led by NQEs have an immediate effect on the underlying electronic structure. Using the MD structural configurations achieved with the rVV10 functional, we calculate the electronic density of states (DOS) of liquid water with the Perdew-Burke-Ernzerhof (PBE) functional [66]. As shown in Fig. 2,

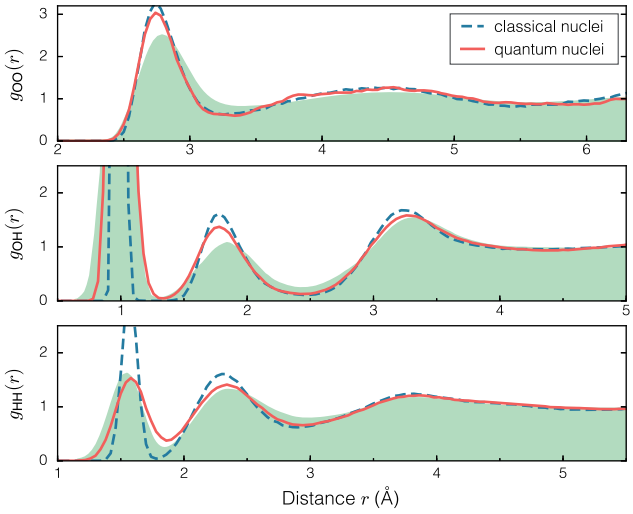

FIG. 1. Radial distribution functions (oxygen-oxygen g_{OO}, oxygen-hydrogen g_{OH}, and hydrogen-hydrogen g_{HH}) with classical (dashed) or quantum (solid) nuclei at room temperature. The dispersion-corrected rVV10 functional is used throughout. Experimental data (shaded) from Refs. [64] (g_{OO}) and [65] (g_{OH} and g_{HH}).

the DOS is broadened upon the inclusion of NQEs, as has been observed previously [67,68]. More relevantly, the VBM and the CBM are shifted by 0.2–0.3 eV, leading to a band-gap renormalization of 0.5 eV (at 300 K) due to quantum fluctuations. As we inspect closely the localization of the VBM and CBM measured by their respective inverse participation ratio (IPR) [69] (cf. Fig. 3), it is clear

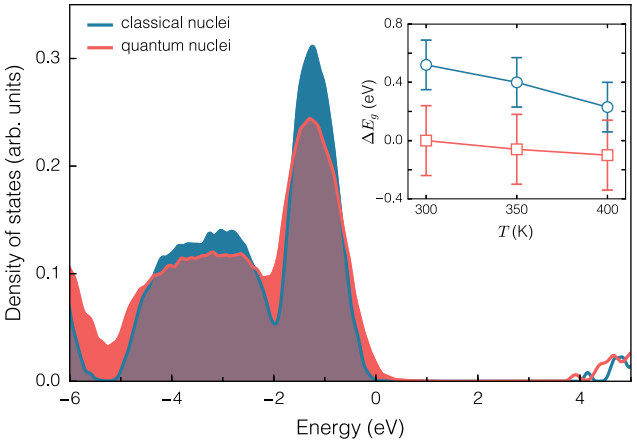

FIG. 2. Electronic density of states of water with classical (blue) or quantum (red) nuclei obtained with the PBE functional (with a $2 \times 2 \times 2$ **k**-point mesh). The structural configurations are generated with the rVV10 functional at 300 K. The closed (empty) region represents the valence (conduction) band. The O-2s peak ($2a_1$, not shown) is used to align the calculations. Energies are referred to the VBM of quantum water. The inset shows the temperature dependence of the band gap obtained with classical (blue circles) or quantum (red squares) nuclei. Values are given relative to the band gap at 300 K with quantum nuclei. Statistical error bars are indicated.

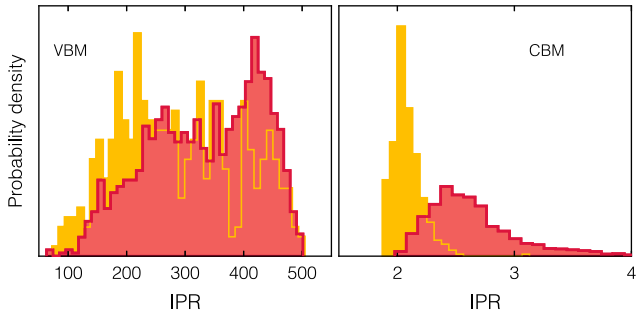

FIG. 3. Probability distribution of the inverse participation ratio (IPR) for the VBM and CBM calculated with their respective PBE eigenstates, with (red) and without (orange) NQEs. A higher IPR indicates stronger localization.

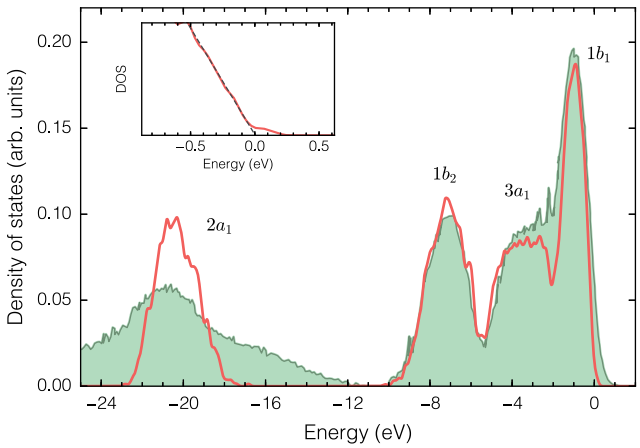

FIG. 4. Density of states of the valence band calculated with QS$GW + f_{\mathrm{xc}}$ (solid line) versus the experimental photoemission spectra (shaded) of Winter *et al.* [5]. NQEs are included in the calculation. The $1b_1$ peak is used to align the calculation and the experiment. The inset shows the VBM as determined by the linearly extrapolated photoemission threshold. Energies are referred to the VBM.

that NQEs shift the IPR to a higher value, thereby increasing the localization for both band-edge states. The stronger localization is consistent with the reduced band gap as the more localized band-edge tails move toward midgap.

Earlier studies suggest that an artificially elevated temperature (usually by 30 to 50 K) can be used to mimic the quantum effects on the structural and diffusion properties of water [27,70,71]. Our calculations show that, as the temperature is raised by 50 K, the band gap of liquid water with classical nuclei decreases by 0.2 eV (cf. Fig. 2). Thus, thermal fluctuations alone do not suffice to recover the band-gap renormalization found with the quantum nuclei. Indeed, we find that the proton-transfer coordinate distribution [28] at 400 K is only marginally broadened compared to what has been observed at 300 K (see the Supplemental Material [49]), and there is no sign of a delocalized hydrogen-bond distribution around $\delta_{\mathrm{OH}} = 0$. Figure 2 (inset) further reveals that the temperature dependence is considerably suppressed in the presence of quantum fluctuations. The band gap decreases by no more than 0.1 eV as the temperature goes from 300 K to 400 K. The band-gap renormalization depicted in Fig. 2 clearly shows that quantum effects are more prominent at lower temperatures.

It is apparent from the DOS in Fig. 2 that the band gap given by the PBE functional is too small. To go beyond the semilocal DFT, we apply the quasiparticle self-consistent QSGW to determine the electronic structure of liquid water, more specifically the band gap and the band-edge positions. Notably, we include vertex corrections in the screened interaction W through a two-point exchange-correlation kernel f_{xc} in the bootstrap approximation [41], and dub the method QS$GW + f_{\mathrm{xc}}$. In the original implementation [40], f_{xc} is determined self-consistently, starting from the inverse dielectric function ε^{-1} in the random-phase approximation (RPA) and iterating until convergence is reached. For bulk materials, we find that the effect of f_{xc} is dominated by the head of the matrix element (i.e., with the reciprocal lattice vector $\mathbf{G} = 0$) [49]. Using only the head, we may write f_{xc} without going through iterations:

$$f_{\mathrm{xc},\mathbf{00}}^{\mathrm{boot}} = \frac{1}{2}\left(\frac{2}{\chi_{\mathbf{00}}^{0}} - v_{\mathbf{0}}\right) + \frac{1}{2}\sqrt{\left(\frac{2}{\chi_{\mathbf{00}}^{0}} - v_{\mathbf{0}}\right)^{2} - \frac{4}{(\chi_{\mathbf{00}}^{0})^{2}}}, \quad (1)$$

where $\chi_{\mathbf{00}}^{0}$ is the head of the independent-particle polarizability, and $v_{\mathbf{0}}$ is the long-range ($\mathbf{G} = 0$) contribution of the bare Coulomb interaction. The use of Eq. (1) is particularly appealing as it brings negligible overhead to standard GW calculations within the RPA. All GW calculations are performed with the ABINIT code [72]. We use a cutoff of 12 Ry and 2000 bands for the calculation of ε^{-1} and the self-energy. The reported quasiparticle energies correspond to the limit of an infinite number of bands [49].

Figure 4 shows the valence band DOS of liquid water obtained with the full-fledged QS$GW + f_{\mathrm{xc}}$ calculations on structural configurations obtained with path-integral MD simulations (averaged over 20 samples per bead uniformly distributed along the entire trajectory). The overall agreement with the UV photoemission spectra of Winter *et al.* [5] is excellent. The binding energies relative to the $1b_1$ peak ($3a_1$ at −2.3 eV, $1b_2$ at −6.2 eV, and $2a_1$ at −19.5 eV) well reproduce the photoemission experiment (−2.3, −6.2, and −19.7 eV, respectively) [5]. The peak widths, which are sensitive to quantum fluctuations, also agree reasonably well with experiment. Note that the experimental $2a_1$ feature is accompanied by a broad background, the origin of which has experimentally been assigned to the energy loss of the initial $1b_1$ electrons [5,73], an effect that is not accounted for in our calculations.

Having identified the electronic structure of the valence manifold, we calculate the band gap of liquid water as the quasiparticle energy difference between the VBM and the CBM. We note that the position of the VBM is here determined as the linearly extrapolated threshold (cf. Fig. 4).

TABLE I. Band gaps (eV) of liquid water calculated with the DFT-PBE functional and various GW schemes. The structural configurations are generated at 300 K with either classical or quantum nuclei. The band-gap renormalization upon the inclusion of NQEs is denoted Δ(NQE). The one-shot G_0W_0 uses the PBE starting point. In the QSGW_0, the screening is fixed at the PBE level. The standard deviation obtained in the PBE also applies to the GW results. All energies are in eV.

	Classical	Quantum	Δ(NQE)
PBE	4.36 ± 0.17	3.86 ± 0.26	−0.50
G_0W_0	8.0	7.3	−0.7
QSGW_0	8.9	8.2	−0.7
QSGW	10.5	9.8	−0.7
QS$GW + f_{xc}$	9.6	8.9	−0.7

This is more robust than simply taking the highest occupied state for liquid water as the extrapolation leads to a faster convergence with supercell size [54]. With the current model of 32 water molecules, the extrapolated value is 0.1 eV above the average highest occupied state. Table I shows the band gap of liquid water calculated with QS$GW + f_{xc}$, DFT-PBE, and various other GW schemes. Our QS$GW + f_{xc}$ gives a band gap of 8.9 eV, in agreement with the experimental estimate of 8.7 eV. We emphasize that this level of agreement can only be achieved in the presence of hydrogen-bond quantum fluctuations; otherwise, the band gap will be too large. Other approaches, such as the PBE and G_0W_0 (on top of the PBE functional) approaches, clearly underestimate the band gap irrespective of the treatment of the nuclei. QSGW without vertex corrections gives a too large band gap even if NQEs are accounted for, in accordance with the general observations that QSGW overshoots the band gap of solid systems [21,40] due to the underscreened W. Replacing W by W_0 calculated at the PBE level, as in the QSGW_0 scheme, generally shows improvement [40]. Nevertheless, the seemingly good agreement with the experimental band gap obtained with QSGW_0 is a result of a fortuitous counterbalance between the overscreened W_0 and the lack of NQEs. The renormalization due to NQEs is about 0.7 eV for all the GW calculations, only slightly higher than in the PBE calculation. This result confirms the generality of NQEs on the electronic structure of liquid water.

The band-lineup problem at photocatalytic interfaces requires the knowledge of the absolute band-edge positions [74]. To this end, we further align the band-edge positions of liquid water to vacuum making use of the computational standard hydrogen electrode (SHE) [10]. The calculation details of the SHE are described in Refs. [54,75]. Once the band-edge positions are determined relative to the SHE, the alignment with respect to vacuum is trivially given by the experimental alignment of the SHE with respect to the vacuum level [76]. The calculated band-edge alignment within the GW approximation is illustrated in Fig. 5. It is evident that the VBM of liquid water shows a strong dependency on the adopted GW scheme. Our QS$GW + f_{xc}$ calculation with

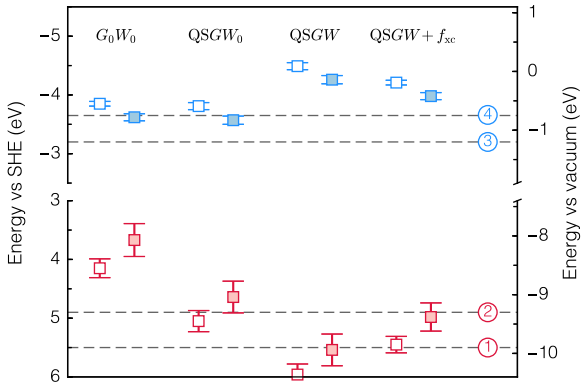

FIG. 5. The VBM (lower panel) and the CBM (upper panel) of liquid water referred to the standard hydrogen electrode (SHE) and to vacuum. The results obtained with quantum (classical) nuclei are marked by closed (open) squares with statistical error bars indicated. Experimental values are indicated by dashed lines with numbered labels (①, Ref. [5]; ②, Ref. [3]; ③, Refs. [6,7]; ④, Ref. [8]).

NQEs places the VBM at −9.4 eV with respect to the vacuum level. This agrees with the assignment of Watanabe *et al.* through UV photoemission spectroscopy [3]. Note that, if the photocurrent were extrapolated with a power law [14], the more recent work of Winter *et al.* [5] would have led to the value of −9.3 eV, rather than the reported −9.9 eV. As for the CBM, its position is found at −0.5 eV (versus vacuum), close to the value of −0.74 eV proposed by Bernas *et al.* [8]. This agreement substantiates the hypothesis that the feature observed at −1.2 eV [6,7] actually corresponds to trapped excess electrons. Our result further implies a trap depth of about 0.7 eV for the hydrated electron.

We remark that our water configurations underlying the electronic-structure calculations are still overstructured to some extent, in particular for g_{OO} (cf. Fig. 1). It is envisaged that an improved description of g_{OO}, possibly through more elaborate MD simulations with hybrid functionals [71] or nonlocal correlations [68], might lead to a smaller band gap as the structure becomes more disordered. Such a structural effect is however marginal, typically on the order of 0.1 eV for the band gap and the band-edge positions, as we have observed [75].

The present work reinforces the efficacy of QSGW with the bootstrap-kernel vertex corrections for realistic systems. In particular, the excellent agreement with the experimental band gap of liquid water is consistent with the high accuracy achieved for various semiconductors and insulators [40]. The benchmarking of band-edge positions is generally less well established, but the good agreement with experiment found here for liquid water is promising and generally consistent with the fact that additional vertex corrections in the self-energy are not critical in ionic systems [77]. Further validation of the role of vertex corrections on the band edges of liquid water awaits the application of more sophisticated methods.

To conclude, our *ab initio* description of the electronic structure of liquid water explicitly takes into account many-body effects and nuclear quantum effects. Accurate self-consistent *GW* calculations are made feasible for liquid water thanks to the highly efficient implementation of vertex corrections based on the bootstrap approximated exchange-correlation kernel. We have underscored the importance of nuclear quantum effects in renormalizing the band gap, a general qualitative effect that is found to persist at the *GW* level. Our calculations lead to a band gap of 8.9 eV, associated with band-edge positions at −9.4 eV (VBM) and −0.5 eV (CBM) with respect to the vacuum level.

We thank Michele Ceriotti for discussions and for access to the private branch of i-PI. Financial support is gratefully acknowledged from the Swiss National Science Foundation (SNSF) (Grants No. 200020-134600 and No. 200020-152799). This work has been performed within the context of the National Center of Competence in Research (NCCR): Materials' Revolution: Computational Design and Discovery of Novel Materials (MARVEL) of the SNSF. Allocations of computational resources at Swiss National Supercomputing Centre (CSCS) is acknowledged.

*wei.chen@epfl.ch

[1] M. Grätzel, Nature (London) **414**, 338 (2001).
[2] M. G. Walter, E. L. Warren, J. R. McKone, S. W. Boettcher, Q. Mi, E. A. Santori, and N. S. Lewis, Chem. Rev. **110**, 6446 (2010).
[3] I. Watanabe, J. B. Flanagan, and P. Delahay, J. Chem. Phys. **73**, 2057 (1980).
[4] P. Delahay and K. V. Burg, Chem. Phys. Lett. **83**, 250 (1981).
[5] B. Winter, R. Weber, W. Widdra, M. Dittmar, M. Faubel, and I. V. Hertel, J. Phys. Chem. A **108**, 2625 (2004).
[6] D. Grand, A. Bernas, and E. Amouyal, Chem. Phys. **44**, 73 (1979).
[7] A. Bernas, D. Grand, and E. Amouyal, J. Phys. Chem. **84**, 1259 (1980).
[8] A. Bernas, C. Ferradini, and J.-P. Jay-Gerin, Chem. Phys. **222**, 151 (1997).
[9] K. Laasonen, M. Sprik, M. Parrinello, and R. Car, J. Chem. Phys. **99**, 9080 (1993).
[10] C. Adriaanse, J. Cheng, V. Chau, M. Sulpizi, J. VandeVondele, and M. Sprik, J. Phys. Chem. Lett. **3**, 3411 (2012).
[11] L. Hedin, Phys. Rev. **139**, A796 (1965).
[12] V. Garbuio, M. Cascella, L. Reining, R. Del Sole, and O. Pulci, Phys. Rev. Lett. **97**, 137402 (2006).
[13] D. Lu, F. Gygi, and G. Galli, Phys. Rev. Lett. **100**, 147601 (2008).
[14] T. A. Pham, C. Zhang, E. Schwegler, and G. Galli, Phys. Rev. B **89**, 060202 (2014).
[15] N. Kharche, J. T. Muckerman, and M. S. Hybertsen, Phys. Rev. Lett. **113**, 176802 (2014).
[16] D. Opalka, T. A. Pham, M. Sprik, and G. Galli, J. Chem. Phys. **141**, 034501 (2014).
[17] C. Fang, W.-F. Li, R. S. Koster, J. Klimes, A. van Blaaderen, and M. A. van Huis, Phys. Chem. Chem. Phys. **17**, 365 (2015).
[18] D. Opalka, T. A. Pham, M. Sprik, and G. Galli, J. Phys. Chem. B **119**, 9651 (2015).
[19] S. V. Faleev, M. van Schilfgaarde, and T. Kotani, Phys. Rev. Lett. **93**, 126406 (2004).
[20] M. van Schilfgaarde, T. Kotani, and S. Faleev, Phys. Rev. Lett. **96**, 226402 (2006).
[21] M. Shishkin, M. Marsman, and G. Kresse, Phys. Rev. Lett. **99**, 246403 (2007).
[22] F. Bruneval and M. Gatti, in *First Principles Approaches to Spectroscopic Properties of Complex Materials*, Topics in Current Chemistry, Vol. 347, edited by C. Di Valentin, S. Botti, and M. Cococcioni (Springer, Berlin Heidelberg, 2014), pp. 99–135.
[23] A. Wallqvist and B. Berne, Chem. Phys. Lett. **117**, 214 (1985).
[24] R. A. Kuharski and P. J. Rossky, J. Chem. Phys. **82**, 5164 (1985).
[25] M. Benoit, D. Marx, and M. Parrinello, Nature (London) **392**, 258 (1998).
[26] D. Marx, M. E. Tuckerman, J. Hutter, and M. Parrinello, Nature (London) **397**, 601 (1999).
[27] J. A. Morrone and R. Car, Phys. Rev. Lett. **101**, 017801 (2008).
[28] M. Ceriotti, J. Cuny, M. Parrinello, and D. E. Manolopoulos, Proc. Natl. Acad. Sci. U.S.A. **110**, 15591 (2013).
[29] M. Ceriotti, W. Fang, P. G. Kusalik, R. H. McKenzie, A. Michaelides, M. A. Morales, and T. E. Markland, Chem. Rev. **116**, 7529 (2016).
[30] S. Zollner, M. Cardona, and S. Gopalan, Phys. Rev. B **45**, 3376 (1992).
[31] M. Cardona and M. L. W. Thewalt, Rev. Mod. Phys. **77**, 1173 (2005).
[32] R. Ramírez, C. P. Herrero, and E. R. Hernández, Phys. Rev. B **73**, 245202 (2006).
[33] R. Ramírez, C. P. Herrero, E. R. Hernández, and M. Cardona, Phys. Rev. B **77**, 045210 (2008).
[34] A. Marini, Phys. Rev. Lett. **101**, 106405 (2008).
[35] F. Giustino, S. G. Louie, and M. L. Cohen, Phys. Rev. Lett. **105**, 265501 (2010).
[36] E. Cannuccia and A. Marini, Phys. Rev. Lett. **107**, 255501 (2011).
[37] S. Poncé, G. Antonius, P. Boulanger, E. Cannuccia, A. Marini, M. Côté, and X. Gonze, Comput. Mater. Sci. **83**, 341 (2014).
[38] G. Antonius, S. Poncé, P. Boulanger, M. Côté, and X. Gonze, Phys. Rev. Lett. **112**, 215501 (2014).
[39] G. Antonius, S. Poncé, E. Lantagne-Hurtubise, G. Auclair, X. Gonze, and M. Côté, Phys. Rev. B **92**, 085137 (2015).
[40] W. Chen and A. Pasquarello, Phys. Rev. B **92**, 041115 (2015).
[41] S. Sharma, J. K. Dewhurst, A. Sanna, and E. K. U. Gross, Phys. Rev. Lett. **107**, 186401 (2011).
[42] S. Habershon, D. E. Manolopoulos, T. E. Markland, and T. F. Miller III, Annu. Rev. Phys. Chem. **64**, 387 (2013).
[43] M. Ceriotti, J. More, and D. E. Manolopoulos, Comput. Phys. Commun. **185**, 1019 (2014).
[44] P. Giannozzi *et al.*, J. Phys. Condens. Matter **21**, 395502 (2009).

[45] M. Ceriotti, G. Bussi, and M. Parrinello, Phys. Rev. Lett. **103**, 030603 (2009).
[46] M. Ceriotti, D. E. Manolopoulos, and M. Parrinello, J. Chem. Phys. **134**, 084104 (2011).
[47] M. Ceriotti and T. E. Markland, J. Chem. Phys. **138**, 014112 (2013).
[48] G. Bussi, D. Donadio, and M. Parrinello, J. Chem. Phys. **126**, 014101 (2007).
[49] See Supplemental Material at http://link.aps.org/supplemental/10.1103/PhysRevLett.117.186401, which includes Refs. [28,50–59], for details on the MD simulation length, the choice of the rVV10 b parameter, enhanced proton transfer with NQEs, and convergence of the GW quasiparticle energies.
[50] I.-C. Lin, A. P. Seitsonen, M. D. Coutinho-Neto, I. Tavernelli, and U. Rothlisberger, J. Phys. Chem. B **113**, 1127 (2009).
[51] G. Miceli, S. de Gironcoli, and A. Pasquarello, J. Chem. Phys. **142**, 034501 (2015).
[52] O. A. Vydrov and T. Van Voorhis, J. Chem. Phys. **133**, 244103 (2010).
[53] R. Sabatini, T. Gorni, and S. de Gironcoli, Phys. Rev. B **87**, 041108 (2013).
[54] F. Ambrosio, G. Miceli, and A. Pasquarello, J. Chem. Phys. **143**, 244508 (2015).
[55] T. Björkman, Phys. Rev. B **86**, 165109 (2012).
[56] P. H. -L. Sit and N. Marzari, J. Chem. Phys. **122**, 204510 (2005).
[57] S. Lebègue, B. Arnaud, M. Alouani, and P. E. Bloechl, Phys. Rev. B **67**, 155208 (2003).
[58] F. Gygi and A. Baldereschi, Phys. Rev. B **34**, 4405 (1986).
[59] W. Chen and A. Pasquarello, Phys. Rev. B **90**, 165133 (2014).
[60] J. Schmidt, J. VandeVondele, I.-F. W. Kuo, D. Sebastiani, J. I. Siepmann, J. Hutter, and C. J. Mundy, J. Phys. Chem. B **113**, 11959 (2009).
[61] J. Wang, G. Romn-Prez, J. M. Soler, E. Artacho, and M.-V. Fernndez-Serra, J. Chem. Phys. **134**, 024516 (2011).
[62] C. Zhang, J. Wu, G. Galli, and F. Gygi, J. Chem. Theory Comput. **7**, 3054 (2011).
[63] I.-C. Lin, A. P. Seitsonen, I. Tavernelli, and U. Rothlisberger, J. Chem. Theory Comput. **8**, 3902 (2012).
[64] A. K. Soper, ISRN Phys. Chem. **2013**, 279463 (2013).
[65] A. K. Soper, Chem. Phys. **258**, 121 (2000).
[66] J. P. Perdew, K. Burke, and M. Ernzerhof, Phys. Rev. Lett. **77**, 3865 (1996).
[67] F. Giberti, A. A. Hassanali, M. Ceriotti, and M. Parrinello, J. Phys. Chem. B **118**, 13226 (2014).
[68] M. Del Ben, J. Hutter, and J. VandeVondele, J. Chem. Phys. **143**, 054506 (2015).
[69] D. Thouless, Phys. Rep. **13**, 93 (1974).
[70] E. Schwegler, J. C. Grossman, F. Gygi, and G. Galli, J. Chem. Phys. **121**, 5400 (2004).
[71] R. A. DiStasio, B. Santra, Z. Li, X. Wu, and R. Car, J. Chem. Phys. **141**, 084502 (2014).
[72] X. Gonze *et al.*, Comput. Phys. Commun. **180**, 2582 (2009).
[73] B. Winter and M. Faubel, Chem. Rev. **106**, 1176 (2006).
[74] R. van de Krol, in *Photoelectrochemical Hydrogen Production*, Vol. 102, edited by R. van de Krol and M. Grätzel (Springer, New York, 2011), pp. 13–67.
[75] F. Ambrosio, G. Miceli, and A. Pasquarello, J. Phys. Chem. B **120**, 7456 (2016).
[76] S. Trasatti, Pure Appl. Chem. **58**, 955 (1986).
[77] A. Grüneis, G. Kresse, Y. Hinuma, and F. Oba, Phys. Rev. Lett. **112**, 096401 (2014).